Contents lists available at ScienceDirect

Biochimica et Biophysica Acta

journal homepage: www.elsevier.com/locate/bbamcr

CrossMark

Sensitivity to anti-Fas is independent of increased cathepsin D activity and adrenodoxin reductase expression occurring in NOS-3 overexpressing HepG2 cells

Clara I. Linares [a], Gustavo Ferrín [a,*,1], Patricia Aguilar-Melero [a], Sandra González-Rubio [a], Manuel Rodríguez-Perálvarez [a], María Sánchez-Aragó [b], Eduardo Chicano-Gálvez [a], José M. Cuezva [b], José L. Montero-Álvarez [a], Jordi Muntané [a,2], Manuel de la Mata [a,1]

[a] Unidad de Gestión Clínica de Aparato Digestivo, Instituto Maimónides de Investigación Biomédica de Córdoba (IMIBIC)/Hospital Universitario Reina Sofía/Universidad de Córdoba, Centro de Investigación Biomédica en Red de Enfermedades Hepáticas y Digestivas (CIBEREHD), Córdoba, Spain
[b] Departamento de Biología Molecular, Centro de Biología Molecular Servero Ochoa, Centro de Investigación Biomédica en Red de Enfermedades Raras (CIBERER), Centro de Investigación Hospital 12 de Octubre, ISCIII, Universidad Autónoma, Madrid, Spain

ARTICLE INFO

ABSTRACT

Stable overexpression of endothelial nitric oxide synthase (NOS-3) in HepG2 cells (4TO-NOS) leads to increased nitro-oxidative stress and upregulation of the cell death mediators p53 and Fas. Thus, NOS-3 overexpression has been suggested as a useful antiproliferative mechanism in hepatocarcinoma cells. We aimed to identify the underlying mechanism of cell death induced by NOS-3 overexpression at basal conditions and with anti-Fas treatment. The intracellular localization of NOS-3, the nitro-oxidative stress and the mitochondrial activity were analysed. In addition, the protein expression profile in 4TO-NOS was screened for differentially expressed proteins potentially involved in the induction of apoptosis. NOS-3 localization in the mitochondrial outer membrane was not associated with changes in the respiratory cellular capacity, but was related to the mitochondrial biogenesis increase and with a higher protein expression of mitochondrial complex IV. Nitro-oxidative stress and cell death in NOS-3 overexpressing cells occurred with the expression increase of pro-apoptotic genes and a higher expression/activity of the enzymes adrenodoxin reductase mitochondrial (AR) and cathepsin D (CatD). CatD overexpression in 4TO-NOS was related to the apoptosis induction independently of its catalytic activity. In addition, CatD activity inhibition by pepstatin A was not effective in blocking apoptosis induced by anti-Fas. In summary, NOS-3 overexpression resulted in an increased sensitivity to anti-Fas induced cell death, independently of AR expression and CatD activity.

© 2015 Elsevier B.V. All rights reserved.

1. Introduction

Nitric oxide (NO) is a lipophilic, highly diffusible and short-lived physiological messenger, which regulates a variety of important biological processes such as vasodilation, respiration, cell migration, immune response and apoptosis. NO is produced within cells by nitric oxide synthase (NOS) using L-arginine as substrate, resulting in the formation of L-citrulline and the end products of NO oxidation, nitrite and nitrate [1]. There are three isoforms of NOS: neuronal (nNOS or NOS-1), inducible (iNOS or NOS-2) and endothelial (eNOS or NOS-3). All of them share similar structures and catalytic modes, but they show different mechanisms regulating their expression and activities [2]. In addition, a new NOS isoform was found in the mitochondria, but whether it corresponds to one of the known isoforms is a matter of discussion [3–5].

The expression of NOS isoforms, including those constitutively expressed, may be triggered by different stimuli and in a tissue-dependent manner. In the liver, NO can be synthesized by the activity of any of the NOS isoforms [6], but its role is an issue of debate. NO is

a mediator of liver injury, but also able to protect against hepatocellular damage, depending on factors such as its concentration or the generating source. Furthermore, the liver expression of NOS isoforms and the NO production have been related to cancer development through pro-/anti-apoptotic activities. NOS-3 may be overexpressed in different types of tumours, and may modulate several cancer-related events such as angiogenesis, apoptosis, cell cycle, invasion or metastasis [1]. By contrast, NOS-3 activation has also been associated with the inhibition of growth and proliferation of hepatoma cells [7]. The molecular mechanism by which NO exerts this antitumoural activity has been related to the inhibition of the mitochondrial electron transport chain and to the induction of nitro-oxidative stress [8,9].

We have previously reported that the NOS-3 overexpression in a hepatocarcinoma cell line is related to apoptosis induced by nitro-oxidative stress and up-regulation of p53 oncoprotein and cell death receptor Fas (or CD95) [10]. Furthermore, the pharmacological modulation of the Fas/Fas ligand (FasL or CD95L) signalling machinery has been suggested as a useful therapeutic strategy, but caution is warranted because administration of agonistic Fas-specific antibodies [11] or FasL [12] causes extensive hepatocyte apoptosis and fatal hepatitis in mice. The increase of Fas-mediated apoptosis may be a promising anticancer therapy in liver disease [10]. In addition, NO-donor molecules have shown antitumoral properties in vitro and in vivo [10,13].

In this study, we aimed to investigate the mechanism by which the stable overexpression of NOS-3 induces cell death in the hepatocarcinoma cell line HepG2, both in basal conditions and with anti-Fas treatment.

2. Material and methods

2.1. NOS-3 overexpression and culture conditions

The cell line with stable overexpression of NOS-3 (4TO-NOS) and its corresponding control cell line (4TO) were obtained and maintained as described elsewhere [14,10]. The cell culture medium was supplemented with 2.5 mM L-arginine to ensure the NOS substrate availability. Cells were seeded to a confluence of 150,000 cells/cm^2, and the measurements were carried out after 48 h. The cell death-inducing agent anti-Fas (Anti-Human Fas or CD95; 0.5 μg/ml. MBL, Nagoya, Japan) was administered 48 h after seeding the cells. Cells were collected 2 h later. The cell-permeable NOS inhibitor N$^{\omega}$-Nitro-L-arginine methyl ester hydrochloride (L-NAME; 5 mM. Sigma-Aldrich, Missouri, USA) and the cathepsin D inhibitor pepstatin A (20 μM or 50 μM; Santa Cruz Biotechnology, California, USA) were added to the culture medium 24 h after seeding the cells.

2.2. NOS-3 subcellular distribution

For western blot localization analysis, the mitochondrial fraction was isolated by ultracentrifugation in a discontinuous sucrose gradient performed with 0.8, 1.0, 1.2, 1.4 and 1.6 M sucrose concentrations in 2 mM HEPES buffer pH 7.4. This method allows for an efficient purification of the mitochondrial fraction and minor contamination with endoplasmic reticulum [15]. Then, mitochondria were subjected to enzymatic digestion with trypsin (6 or 20 μg/100 μg protein) or proteinase-K (10 or 40 μg/100 μg protein). 10 μg of protein was separated by SDS–PAGE, electroblotted onto nitrocellulose membrane, and sequentially probed with specific antibodies against MTCO2 (a protein from the inner mitochondrial membrane) (Life Technologies), translocase of outer mitochondrial membrane 40 homolog (TOM40) and NOS-3 (Santa Cruz Biotechnology). The cellular localization of the NOS-3 protein was additionally assessed by using a confocal microscope (LSM 5 Exciter) and a confocal imaging system (ZEN 2008, Carl Zeiss, Jena, Germany). Cells were fixed and incubated with the primary antibodies anti-NOS-3 (Santa Cruz Biotechnology) and anti-MTCO2 (Abcam, Cambridge, UK). Secondary conjugated antibodies were Alexa

Fluor 488 and 594 (Life Technologies, California, USA). The specificity of the immunoreactivity was verified by incubating cells without the primary antibodies. ImageJ software was used to assess the mitochondrial localization of NOS-3 (http://imagej.nih.gov/ij/).

2.3. Oxygen consumption

O$_2$ consumption determinations in intact cells or in digitonin-permeabilized cells were carried out in an oxygraph with a Clark electrode (Hansatech Instruments, Norfolk, UK) [16]. Briefly, 5×10^6 cells were trypsinized, counted and resuspended in culture medium or respiration buffer (10 mM MgCl$_2$, 250 mM Sucrose, 20 mM HEPES pH 7.4, 1 mM ADP, 2 mM KH$_2$PO$_4$), respectively. Oxygen consumption was measured at 37 °C with stirring. 6.25 μM FCCP was used to uncouple respiration in intact cells. For polarographic measurements, cells were permeabilized with 1% digitonin (1.2 μl/10^6 cells) and the oxygen consumption was recorded after the addition of substrates and inhibitors for complex I (5 mM Glutamate plus Malate, 2 μM Rotenone), complex II + III (5 mM Succinate plus Glyceraldehyde-3-P, 0.1 μM Antimycin A) and complex IV (1.2 mM TMPD, 6 mM KCN).

2.4. Mitochondrial membrane potential

The mitochondrial membrane potential (MMP) was monitored by using the potential-sensitive fluorescent probe tetramethyl-rhodamine methyl ester (TMR) (Life Technologies). Briefly, cells were washed with PBS and further incubated with 10 μM TMR for 20 min. The registration of the measurement was started with the addition of 5 mM glucose. The fluorescence emitted by TMR ($\lambda_{ex} = 550$ nm, $\lambda_{em} = 570$ nm) was detected in situ using a GENios Microplate Reader (TECAN, Männedorf, Switzerland).

2.5. Quantitative analysis of protein nitration

The quantification of protein nitration as a measurement of reactive nitrogen species (RNS) was determined in the mitochondrial fraction by western blot. The post-translational modification 3-nitrotyrosine was used for this purpose. The protein samples were separated by SDS–PAGE in non-reducing conditions, transferred to nitrocellulose membrane, and probed with an anti-3-nitrotyrosine primary antibody (Sigma-Aldrich) [10]. The data from the densitometry analysis of the 55 kDa protein band were normalized to a total protein value of 10 μg.

2.6. Nitric oxide production

NO production was determined by the Griess reaction as we previously described [14]. NO-related end products nitrates and nitrites were quantified in the cell culture medium 2 h after anti-Fas administration. Nitrite concentrations were accurately determined by a nitrite calibration curve.

2.7. Determination of mitochondrial reactive oxygen species

Cellular reactive oxygen species (ROS) were detected by using the fluorescent probes 2,7-dichlorofluorescein-diacetate (DCFDA) and dihydroethidium (DHE) (Life Technologies). The cells were washed and then incubated with 10 μM DCFDA or 5 μM DHE for 20 min or 10 min, respectively. Measurements were initiated by the addition of 5 mM glucose. The fluorescence emitted by DHE ($\lambda_{ex} = 510$ nm, $\lambda_{em} = 590$ nm) and DCFDA ($\lambda_{ex} = 500$ nm, $\lambda_{em} = 520$ nm) was assessed in situ using a microplate reader. DHE was not used with L-NAME because the NOS inhibitor appeared to interact with the probe (data not shown).

2.8. Gene expression analysis and mitochondrial DNA copy number quantification

The expression analysis of the antioxidant and pro-apoptotic genes was determined by RT–qPCR using a LightCycler 480 System (Roche, Basel, Switzerland) and the One-Step QuantiTect SYBR-Green Kit (Qiagen, Limburg, Netherlands). Total cellular RNA was extracted by using TRIsure reagent (Bioline, London, UK), treated with RNAse-Free DNase (Promega, Wisconsin, USA), and used as template for mRNA amplification with specific human oligodeoxynucleotides designed by Primer3 software (v.0.4.0). The expression of ribosomal protein L13A (RPL13A) was used as a reference gene. The primer sequences and positions into the cDNA are summarized in Table 1. The RNA concentration and its integrity were confirmed by standard procedures. The PCR reaction was performed in duplicate, by adjusting the annealing temperature to 60 °C and in a final volume of 10 μl.

The mitochondrial DNA (mtDNA) quantification was also performed by RT–qPCR with the ThermOne™ RT-PCR Premix (RBC, Taipei, Taiwan). The total cellular DNA extracted using standard procedures was used as template and was amplified with specific oligodeoxynucleotides for MTCO2 and succinate dehydrogenase subunit A (SDHA), as previously reported [17]. MtDNA copy number per cell was calculated using SDHA amplification as a reference for nuclear DNA content.

2.9. Mitochondrial protein expression analysis

Expression analysis for mitochondrial proteins from respiratory complexes was assessed by western blot. 40 μg from the total cellular proteins was separated by SDS–PAGE, then transferred to nitrocellulose membrane, and finally probed with primary antibodies anti-NDUFB6 (complex I), anti-SDHB (complex II), anti-UQCRC2 (complex III) and anti-MTCO2 (complex IV), respectively (Life Technologies). The densitometry analysis of the lines after Ponceau S staining was used as protein-loading control.

Table 1
List of human primers used for RT–qPCR.

Primer	Gene	Position	Sequence (5′ to 3′)
GPx1-qF	GPX1	301–320	TCGGCTTCCCGTGCAACCAG
GPx1-qR	NM_000581.2	420–440	CGCACCGTTCACCTCGCACTT
GPx4-qF	GPX4	403–422	CCTTCCCGTGTAACCAGTTC
GPx4-qR	NM_002085.3	587–609	ACTTGGTGAAGTTCCACTTGATG
Cat-qF	CAT	1028–1053	TGGTAAACTGGTCTTAAACCGGAATC
Cat-qR	NM_001752.3	1159–1179	GGCGGTGAGTGTCAGGATAGG
Sod1-qF	SOD1	430–451	TGTGGCCGATGTGTCTATTGAA
Sod1-qR	NM_000454.4	519–539	CACCTTTGCCCAAGTCATCTG
Sod2-qF	SOD2	708–728	GGGGAGCACGCTTACTACCTTC
Sod2-qR	NM_001024465.1	845–867	TCTTGCTGGGATCATTAGGGTAT
GSS-qF	GSS	286–308	AGATGGACTTCAACCTGCTAGTG
GSS-qR	NM_000178.2	374–395	GTCAAAGAGACGAGCGGTAAAG
Apaf1-qF	APAF-1	3105–3128	TGGCAGTGGTTGCTTTGTCCCAGT
Apaf1-qR	NM_013229.2	3190–3219	GGAGAAAACATCACACCATGAACC CAACTT
Bax_qF	BAX	229–251	GCGTCCACCAAGAAGCTGAGCGA
Bax_qR	NM_138764.4	401–424	TGCTGGCAAAGTAGAAAAGGGCGA
Bik-qF	BIK	96–118	CTTGATGGAGACCCTCCTGTATG
Bik-qR	NM_001197.4	166–186	AGGGTCCAGGTCCTCTTCAGA
Rpl13A-qF	RPL13A	541–563	CCTGGAGGAGAAGAGGAAAGAGA
Rpl13A-qR	NM_012423.3	642–666	TTGAGGACCTCTGTGTATTTGTCAA

GPX1, Glutathione peroxidase-1; GPX4, Glutathione peroxidase-4; Cat, Catalase; SOD-1, Cu/Zn-Superoxide dismutase; SOD-2, Mn-Superoxide dismutase; GSS, Glutathione synthetase; APAF-1, Apoptotic peptidase activating factor 1; BAX, BCL2-associated X protein; BIK, Bcl-2-interacting killer; RPL13A, Ribosomal protein L13A. Primers were designed using Primer3 software (v.0.4.0).

2.10. Cell death analysis

Cell death was assessed in cell lysates by the release of cytochrome c (cyt c) from the mitochondria, and by the caspase-9 and caspase-3 enzyme activity. The cytoplasmic cyt c release was determined by western blot analysis by using the anti-cyt c primary antibody (Santa Cruz Biotechnology) and anti-β-actin (Abcam) as protein-loading control. Caspase-9/-3 activities were spectrophotometrically measured as previously reported [10].

2.11. Protein expression profiling by two dimensional electrophoresis

Protein samples were obtained in 20 mM Tris–HCl pH 7.6, 0.5 M Sucrose, 0.15 M KCl, 10 μg/ml leupeptin, 2 μg/ml aprotinin, 10 mg/ml PMSF and 20 mM DTT supplemented with the commercial Mini EDTA-free protease inhibitor cocktail (Roche). Proteins were quantified by the Bradford assay and 300 μg of total cellular proteins was used in each isoelectrofocusing (IEF) strip (18 cm ReadyStrip™ IPG Strips pH 3–10 nonlinear). The IEF program and the two dimensional electrophoresis (2-DE) conditions were performed as detailed in [14]. Gels from 2-DE were stained with SYPRO Ruby and further digitalized with the FX ProPlus Multiimager. The analysis of the differential intensity spot and the spot volume, normalized by the total density in gels, was quantified by using the PDQuest software (v.8.0.1) (Bio-Rad Laboratories, California, USA). Protein samples from four independent experiments were run in triplicate.

2.12. Identification of differentially expressed proteins

Differentially expressed protein spots were excised from the preparative 2-D gel by using a ProPic workstation (Genomic Solutions Inc., Michigan, USA), digested with trypsin, and subjected to MALDI-TOF analysis in the UCO-SCAI proteomics facility (Córdoba, Spain. Carlos III Networked Proteomics Platform, ProteoRed-ISCIII) [14]. The confirmation of the results was performed by western blot, using 5 μg of total cellular proteins and the primary antibodies anti-HSP60, anti-PDI, anti-ADX Reductase and anti-PRDX3 (Santa Cruz Biotechnology).

2.13. Cathepsin D activity assay

Cathepsin D activity was measured in cell lysates with the use of a commercial assay kit (Abcam) following the manufacturer recommendations. Data were normalised by the cell number, which was assessed immediately before the enzyme activity measurement.

2.14. Statistical analysis

Results were expressed as mean ± standard error. Data were compared using the non-parametric method Kruskal–Wallis and the Mann–Whitney's U test, searching for differences between groups (n < 30). All tests and calculations were done with the statistical package SPSS 15.0 for Windows (IBM). Statistical difference was set at $p \leq 0.05$. * Indicates statistically significant differences between cell lines for a same condition. # Indicates statistically significant differences between conditions (anti-Fas or L-NAME vs. basal; + L-NAME vs. anti-Fas) for a same cell line.

3. Results

3.1. NOS-3 localizes in the mitochondrion outer membrane

The western blot analysis of NOS-3 in different subcellular fractions showed an expression of the protein in membranes, cytoplasm and mitochondria from 4TO-NOS cells (Fig. 1A). In addition, enzymatic treatment of intact mitochondria with trypsin and proteinase-K efficiently removed NOS-3 and TOM40 from mitochondria, but not
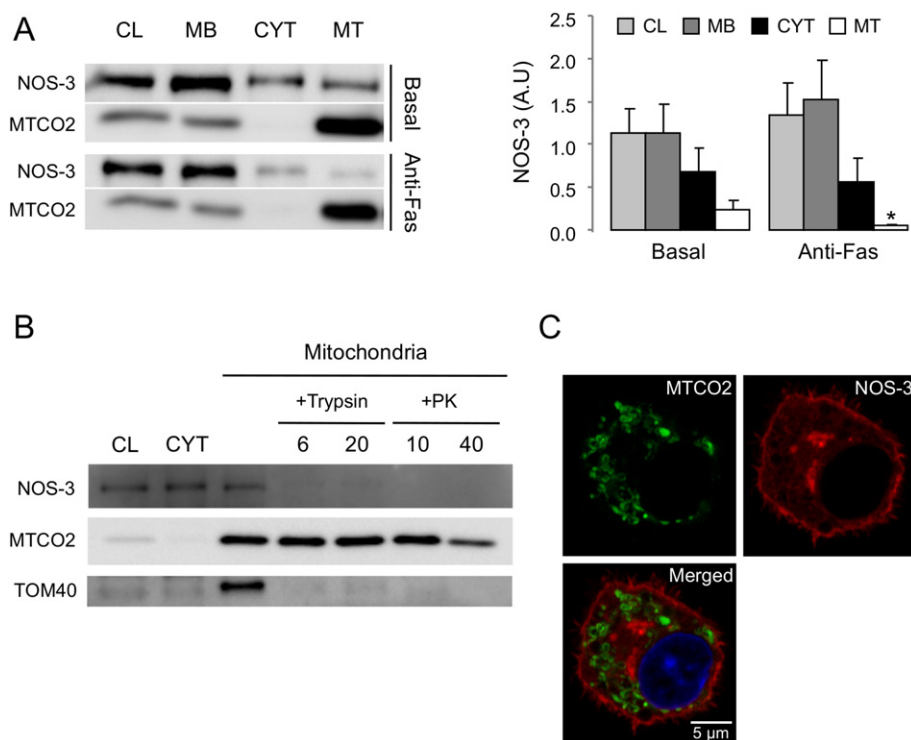
Fig. 1. NOS-3 localization in 4TO-NOS cells. (A) Subcellular localization of NOS-3 in 4TO-NOS. Effect of anti-Fas administration on the mitochondrial localization of NOS-3 (n = 3). Densitometry of the lines corresponding to mitochondrial NOS-3 is shown. MTCO2 signal was used as loading control for cell lysate (CL), membrane fraction (MB) and mitochondrial fraction (MT). NOS-3 signal in cytoplasm (CYT) was referred to the protein load. (B) Mitochondrial localization of NOS-3 assessed by western blot. Mitochondrial fraction was subjected to enzymatic digestion with trypsin (6 or 20 μg/100 μg protein) or proteinase-K (PK, 10 or 40 μg/100 μg protein). (C) NOS-3 cellular localization by confocal microscopy. Green: MTCO2 protein. Red: NOS-3 protein. Blue: DAPI. Statistically significant differences between cell lines* or between treatments# are marked.

MTCOII since the proteases cannot access inner membrane proteins (Fig. 1B). The confocal immunofluorescence study showed that NOS-3 was primarily localized in the plasma membrane and in the cellular cytoplasm of the NOS-3-overexpressing cells (Fig. 1C). The mitochondrial localization of NOS-3 was not confirmed by this approach.

In order to assess the effect of anti-Fas on the subcellular distribution of NOS-3 and cell death susceptibility, we studied the mitochondrial localization of the protein in the presence of the apoptosis inducer. As shown in Fig. 1A, anti-Fas had a trend to an increased NOS-3 expression in 4TO-NOS, which coincided with a reduced localization of the protein in the mitochondrial fraction (0.24 vs. 0.06, p = 0.021).

3.2. Stable overexpression of NOS-3 does not affect the cell respiratory capacity

In order to evaluate the role of NOS-3 overexpression on cellular respiration, we analysed oxygen consumption associated with mitochondrial complexes I (CI), II + III (CII + III) and IV (CIV) in the 4TO-NOS cell line. As shown in Fig. 2, NOS-3 overexpression was related to a subtle increase in respiratory activity of CII + III (119%, p = 0.024), without affecting oxygen consumption dependent of CI and CIV (Fig. 2A). This resulted in a non-significant increase of the endogenous cellular respiratory capacity (Fig. 2B) and in a higher MMP (129%, p = 0.004) (Fig. 2C). When the cell-permeable NOS inhibitor L-NAME was added to the cell culture medium, an increase in oxygen consumption dependent on CI and CII + III, in both 4TO (166% p = 0.014 and 118% p = 0.033, respectively) and 4TO-NOS cell line (154% p = 0.025 and 138% p = 0.052, respectively) was observed (Fig. 2A). The induction of apoptosis by anti-Fas led to a statistically significant decrease in oxygen consumption mostly due to 30% loss of CI activity (p = 0.011), and reduced the endogenous respiratory capacity (5.4 vs. 6.3, p = 0.050) and maximum respiratory capacity (10.1 vs. 12.9, p = 0.050) in

4TO-NOS when compared to 4TO cells (Fig. 2A and B). The simultaneous administration of anti-Fas and L-NAME had a similar effect on oxygen consumption as that caused by the sole addition of L-NAME on 4TO cells. By contrast, in 4TO-NOS, L-NAME inhibited the effect of anti-Fas on the mitochondrial CI (p = 0.053). The oxygen consumption increase induced by L-NAME in the presence of anti-FAS was paralleled by MMP increase in the two cell lines.

3.3. Nitro-oxidative stress and mtDNA copy number are enhanced in 4TO-NOS

The mitochondrial localization of NOS-3 in 4TO-NOS cells was associated with increased levels of tyrosine nitration of mitochondrial proteins (85.48 vs. 35.81, p = 0.050), which translates the production of RNS (Fig. 3A). In addition, NOS-3 overexpressing cells accumulated a higher concentration of nitric oxide end products in the cell culture medium (Fig. 3B), and showed a general ROS production increase (168%, p < 0.001 for DCF; 149%, p = 0.048 for DHE) (Fig. 3C) and an up-regulation of antioxidant genes encoding for proteins superoxide dismutase (SOD)-1 (154%, p = 0.032), SOD-2 (210%, p = 0.019), catalase (149%, p = 0.021), glutathione peroxidase (GPX)-1 (235%, p = 0.032), GPX-4 (155%, p = 0.032) and glutathione synthetase (GSS) (167%, p = 0.034) (Fig. 3D). The administration of L-NAME did not reduce oxidative stress in 4TO-NOS (Fig. 3C), but caused a reduction of mitochondrial protein nitration (Fig. 3A) and a lower accumulation of nitrates and nitrites in the cell culture medium (Fig. 3B), which balanced the observed differences between 4TO-NOS and the control cell line 4TO. The nitro-oxidative stress related to NOS-3 overexpression was associated with an increased mtDNA copy number (148%, p < 0.001) (Fig. 3E) and with a higher protein expression of mitochondrial CIV (163%, p = 0.019) (Fig. 3F).
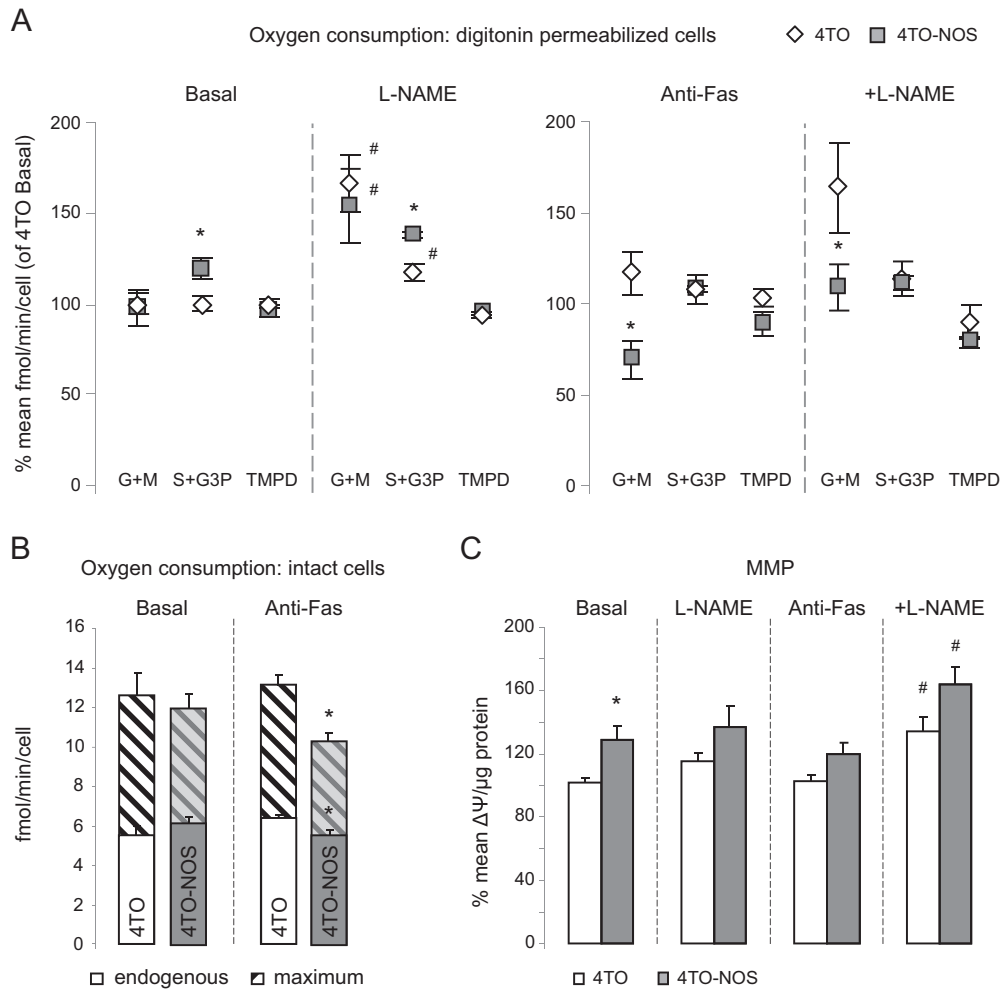
Fig. 2. Oxidative phosphorylation system performance in 4TO-NOS cells. (A) Oxygen consumption of digitonin permeabilized cells in the presence of electron donors for complex I (Glutamate + Malate, G + M), complex II + III (Succinate + G3P, S + G3P) and complex IV (TMPD) (at basal condition: n = 9; with anti-Fas: n = 6 and n = 8 for 4TO and 4TO-NOS cells, respectively; with L-NAME: n = 3; with anti-Fas plus L-NAME: n = 3). (B) Oxygen consumption rate in intact cells (at basal condition: n = 5 and n = 4 for 4TO and 4TO-NOS, respectively; with anti-Fas: n = 3). (C) Mitochondrial membrane potential (n = 7). +L-NAME indicates treatment with anti-Fas plus L-NAME. Data are mean ± SEM. Statistically significant differences between cell lines* or between treatments# are marked.

Anti-Fas led to the accumulation of nitrates and nitrites in the cell culture medium of 4TO-NOS cells (1.25 vs. 4.12, p = 0.034) (Fig. 3B). In addition, anti-Fas induced the antioxidant gene expression in 4TO cells, but it had no additional effect on gene expression and oxidative stress in the 4TO-NOS cell line (Fig. 3C and D).

3.4. NOS-3 overexpression increases susceptibility to anti-Fas-induced cell death

As shown in Fig. 4A, NOS-3 overexpression was associated with an increased expression of pro-apoptotic genes Bax (164%, p = 0.003), Bik (354%, p = 0.002) and Apaf-1 (168%, p = 0.002) at basal conditions. This coincided with a higher localization of cyt c in the cytoplasm (168%, p = 0.019), and the increase of caspase-9 (124%, p = 0.047) and caspase-3 (166%, p = 0.011) associated activities (Fig. 4B and C). The administration of anti-Fas stimulated Bik expression in 4TO (146%, p = 0.010) and 4TO-NOS cells (563%, p = 0.007), without affecting Bax or Apaf-1. In addition, anti-Fas caused an increase in the caspase-3 activity in both cell lines (153% and 318%, respectively; p < 0.050), as well as a higher caspase-9 activity only in 4TO-NOS (229%, p = 0.034). There were no significant differences in the release of cyt c after incubation with anti-Fas.

3.5. Comparative proteomic profile of the 4TO-NOS cell line

The proteomic profile of 4TO-NOS cells was analysed and further compared to that of the control cell line 4TO, searching for differentially expressed proteins that could be involved in the process of ROS production and cell death observed at basal condition. The quantitative analysis of the gels yielded 110 spots with significantly altered expression. 56 of these spots were identified by mass spectrometry as 42 different proteins. The location of these spots in the master gel is shown in Fig. 5A. Supplementary Fig. 1 shows a representative 2-D gel for each condition. Differentially expressed proteins have been classified according to their main biological functions (Table 2). Differences in proteins involved in metabolism (11), cytoskeleton (2), RNA processing (5), protein processing (8), protein degradation (6) and redox homeostasis (10) were found. NOS-3 overexpression mainly affected the expression of proteins involved in metabolism (8) and redox system (8). Among the metabolic proteins, three were up-regulated proteins (+) involved in the β-oxidation and glycolysis processes: medium and short-chain-specific acyl-CoA dehydrogenases (+5.4/+2.8, respectively) and glyceraldehyde-3-phosphate dehydrogenase (GAPDH; +2.3). In the second largest group of proteins deregulated by NOS-3 overexpression, we found over-expression of proteins in both the cell anti-oxidant system and the pro-oxidant system: thioredoxin-dependent peroxide
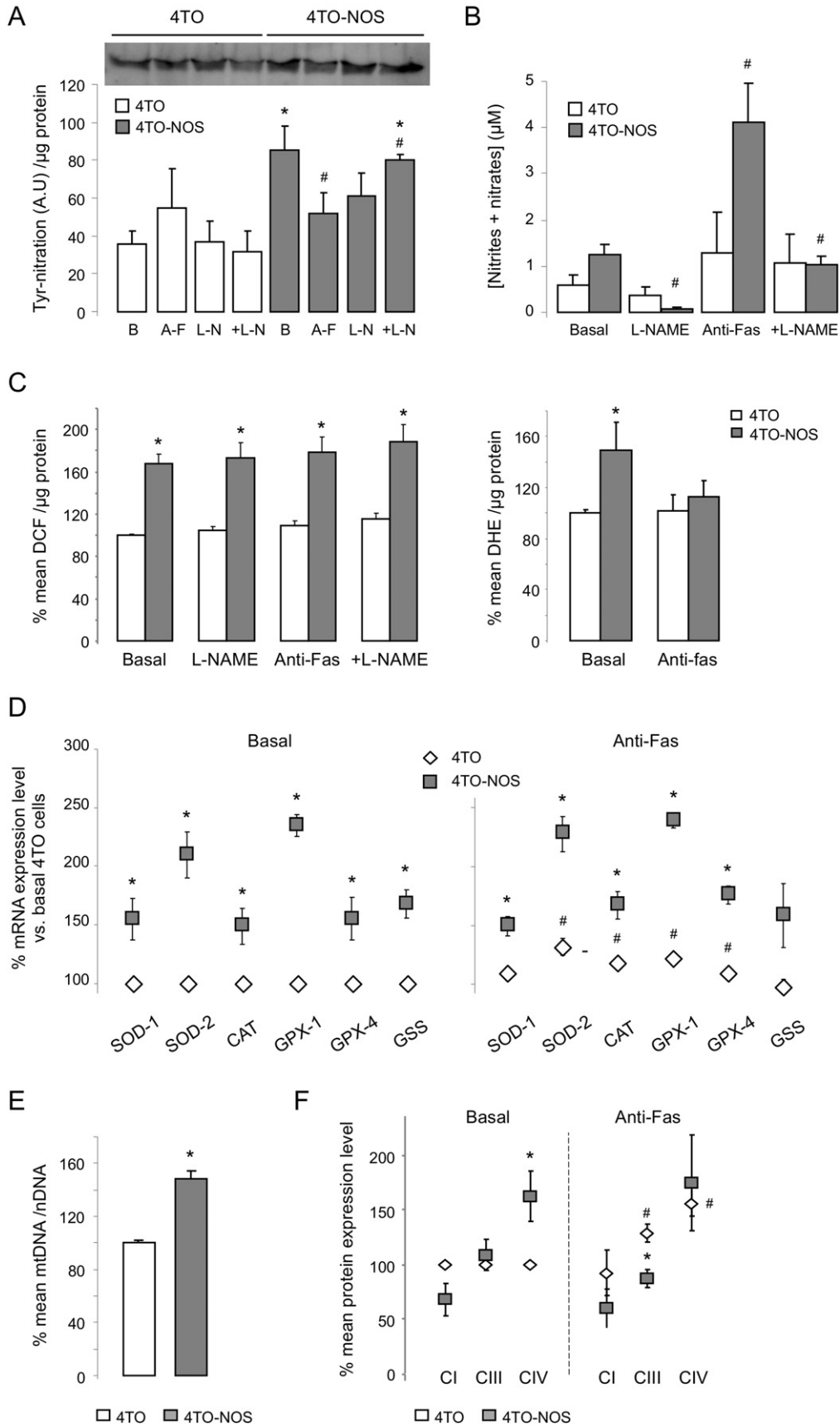
Fig. 3. Effect of NOS-3 overexpression on the cellular nitro-oxidative status and mitochondrial biogenesis. (A) Quantification of protein nitration in the mitochondrial fraction by western blot (n = 3). (B) Accumulation of nitric oxide end products, nitrates and nitrites, in the cell culture medium (n = 3). (C) General ROS production was assessed by using probes DCF (n = 11 for basal and anti-Fas; n = 4 for L-NAME and +L-NAME) and DHE (n = 8). (D) Gene expression analysis of antioxidant proteins GPX-1, GPX-4, Catalase, SOD-1, SOD-2 and GSS (n = 4). (E) MtDNA copy number quantification (n = 9). (F) Expression analysis of proteins from the mitochondrial respiratory complexes (n = 3 or 4). B indicates basal conditions. +L-NAME (+L-N) indicates treatment with anti-Fas (A-F) plus L-NAME (L-N). Data are mean ± SEM. Statistically significant differences between cell lines* or between treatments# are marked.

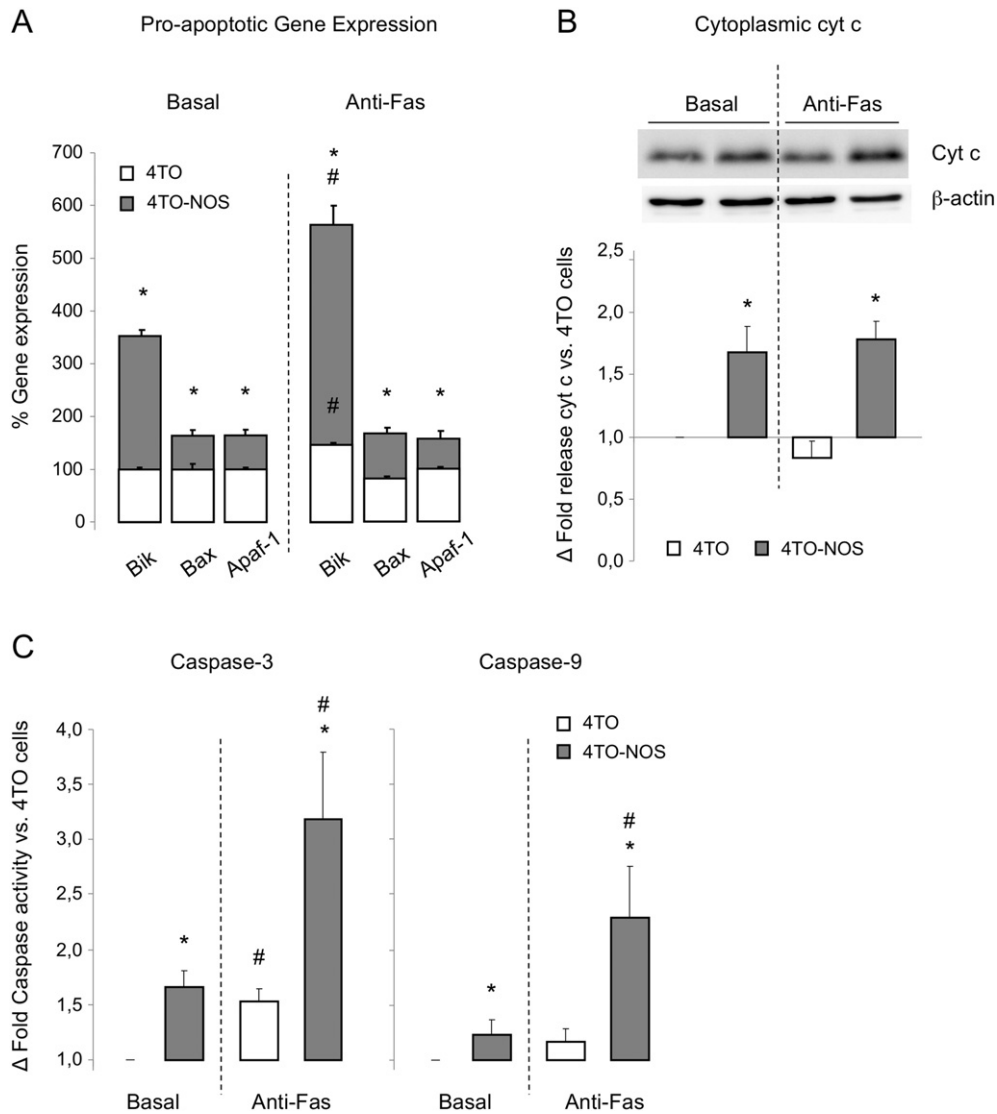**Fig. 4.** Effect of anti-Fas administration on cell death. (A) Gene expression analysis of pro-apoptotic proteins APAF-1, BAX and BIK (n = 4). (B) Cytoplasmic expression of cyt c. It is represented the cyt c/β-actin ratio *versus* the control cell line 4TO at basal condition (n = 3). (C) Caspase-9 and caspase-3-associated activities (n = 4). Data are mean ± SEM. Statistically significant differences between cell lines* or between treatments# are marked.

reductase mitochondrial (PRDX3; +3.2), peroxiredoxin-2 (PRDX2; +2.1), superoxide dismutase [Mn] mitochondrial (SOD2; +3.2) and NADPH:adrenodoxin oxidoreductase mitochondrial (ADX reductase or AR; +3.7). Cathepsin D (CatD) was identified in two different spots as a protease upregulated by NOS-3 overexpression (+2.3 and +1.9), and in a third additional spot that was only detected in 4TO-NOS cells.

In the presence of anti-Fas, the cell lines 4TO and 4TO-NOS showed differences in the protein expression profile as a consequence of NOS-3 overexpression. The differentially expressed proteins were mainly involved in protein processing (6), protein degradation (6) and redox homeostasis (5). The apoptosis inductor did not modify the expression pattern of CatD in 4TO-NOS.

In order to verify 2-D PAGE/MS results, we randomly chose four proteins from those previously identified by MS, and confirmed their relative expression deregulation by western blot analysis. These proteins were heat shock protein 60 (HSP60), protein disulfide isomerase (PDI), PRDX3 and AR (Fig. 5B).

3.6. Cathepsin D expression, but not its activity, is associated with cell death

Next, we investigated the role of CatD in NOS-3 overexpressing cells. As shown in Fig. 6, the overexpression of CatD in 4TO-NOS cells was

accompanied by the increase of its enzymatic activity (176%, p = 0.020) (Fig. 6A). The inhibition of CatD activity by 20 µM pepstatin A (Fig. 6B) had no effect on cell growth (Fig. 6C) but it was associated with the activity increase of caspase-3 (1.23 fold, p = 0.050) and caspase-9 (1.22 fold, p = 0.037) in 4TO-NOS when compared to basal condition (Fig. 6D and E). At 50 µM, pepstatin A caused a significant increase in cell doubling time in the 4TO-NOS cell line (66.2 vs. 47.5, p = 0.021) (Fig. 6F), which was paralleled by a higher caspase-3 activity (1.73 fold increase, p = 0.047) (Fig. 6G). The addition of anti-Fas to the cell culture medium did not affect CatD activity in the cell lines 4TO or 4TO-NOS (Fig. 6A). By contrast, the simultaneous administration of anti-Fas and pepstatin A resulted in the activity increase of caspase-3 (p = 0.050) in the cell line 4TO-NOS when compared to the condition of anti-Fas addition (Fig. 6D).

4. Discussion

We have previously shown that stable NOS-3 overexpression induces the oncoprotein p53 and the cell death receptor Fas, in HepG2 cells as well as in tumours subcutaneously developed in a xenograft mouse model [10]. Indeed NOS-3 up-regulation has been suggested as a candidate antiproliferative mechanism in hepatocarcinoma cells.
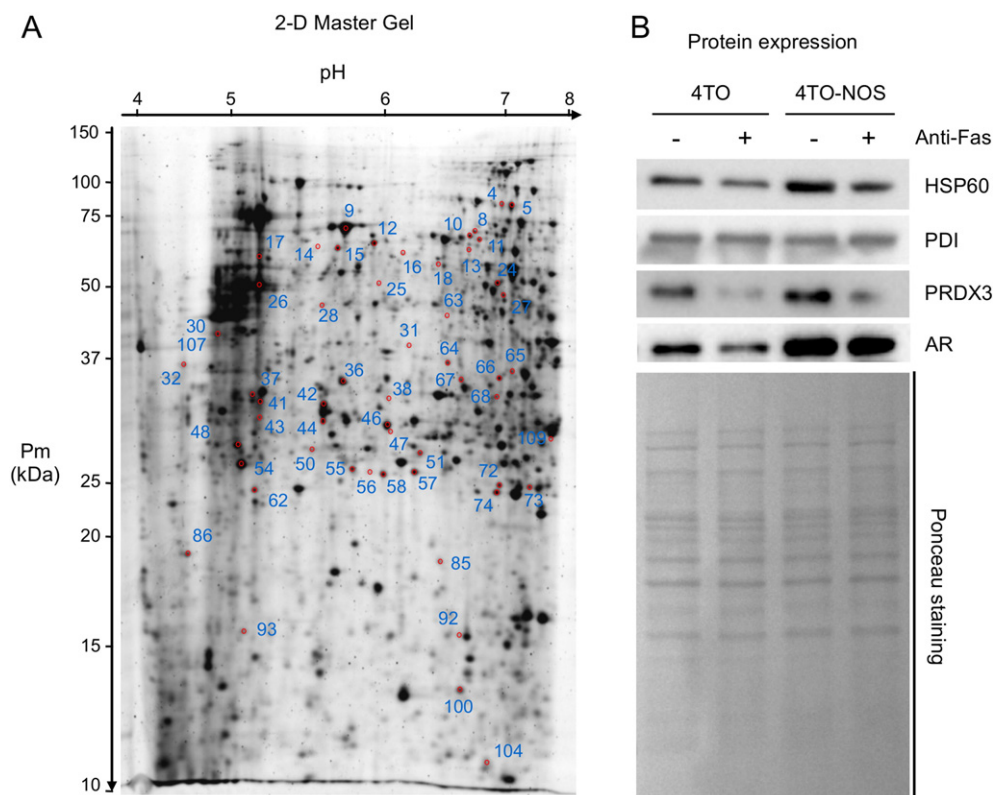
Fig. 5. Differentially expressed proteins in 4TO-NOS cells. (A) 2-D Master gel. Deregulated protein spots in 4TO-NOS are marked and numbered. (B) Western blot analysis of proteins 60 kDa heat shock protein mitochondrial (HSP60), protein disulfide-isomerase (PDI), thioredoxin-dependent peroxide reductase mitochondrial (PRDX3) and NADPH:adrenodoxin oxidoreductase mitochondrial (AR). A representative image of a Ponceau-stained membrane used in the western blot analysis is shown. Data are mean ± SEM. Statistically significant differences between cell lines* or between treatments# are marked.

In the present study, we have investigated the mechanisms involved in cell death promoted by NOS-3 overexpression. In addition, we have explored the susceptibility to anti-Fas-induced cell death in the 4TO-NOS cell line. Fig. 7 summarizes the main findings of this study about cell death mechanisms induced by NOS-3 overexpression in a representative scheme.

As NOS-3 is expressed in mitochondria [3], and it is well known the key role of this organelle in apoptotic cell-death, we analysed the expression pattern of the protein in 4TO-NOS cells. We found that NOS-3 is mainly localized in the plasma membrane and cytoplasm, which agrees with earlier studies in which NOS-3 was present in the Golgi complex and in cell–cell contacts of confluent cells [18]. In addition, we observed that NOS-3 colocalized with mitochondrial proteins, and that NOS-3 was cleaved from the mitochondria by a protease treatment, suggesting its association with the outer mitochondrial membrane. This was consistent with the high levels of tyrosine nitration of mitochondrial proteins observed in NOS-3 overexpressing cells. Due to the inhibitory effect that NO has on the oxidative phosphorylation (OXPHOS) system, its ability to diffuse through cell membranes, and the finding that NOS-3 is localized in the mitochondria, we next investigated the respiratory capacity of the 4TO-NOS cell line. Unexpectedly, NOS-3 overexpression did not cause any relevant effect on the mitochondrial respiration. Despite this, 4TO-NOS cells showed increased levels of oxidative stress that coincided with the expression increase of genes involved in ROS detoxification and with a high mtDNA copy number, compared to the control cell line 4TO. In this regard, previous studies have shown that mtDNA biogenesis may be regulated by oxidative stress under different conditions [19], and that NO is able to trigger mitochondrial biogenesis in culture cells [20]. The increase in mtDNA copy number was paralleled by a higher expression of the mtDNA-encoded protein MTCO2, which may be an attempt by 4TO-NOS cells to adapt to the conditions of NO overproduction.

With the aim to link these previous observations to NOS-3 overexpression, we additionally used L-NAME. This commonly used NOS inhibitor effectively suppressed the effects of NOS-3 overexpression relating to the accumulation of NO end products and the nitration of mitochondrial proteins. However, L-NAME was not effective in suppressing oxidative stress induced by NOS-3 overexpression. Conversely, L-NAME caused an increased activity of the OXPHOS system, which is closely related to ROS production [21] and may be a consequence of the inhibitory effect of NO on the respiration [8]. Nevertheless, L-NAME caused a similar effect in both cell lines 4TO and 4TO-NOS, thus indicating that NOS-3 overexpression has no relevant role in mitochondrial respiration. This result was confirmed when we measured cellular respiration in non-permeabilized cells. Thus, despite the inhibitory effect of NO in respiration, the apoptosis induction by NOS-3 overexpression did not occur through dysfunction of the OXPHOS system.

We have previously shown that 4TO-NOS cell line has increased levels of p53 protein [10], which is an important cell cycle regulator able to initiate apoptosis in response to oxidative stress [22]. Indeed, p53 activity has been related to the expression regulation of several apoptotic genes [23]. In the present study, NOS-3 overexpression was associated with the expression increase of pro-apoptotic genes such as Bax, Bik and Apaf-1, and with a consequent release of cyt c into the cytoplasm and the activity increase of caspase-9 and caspase-3. These results would explain the spontaneous apoptosis showed by 4TO-NOS at basal condition. In addition, NOS-3 overexpression was related to MMP increase, consistent with the induction of apoptosis through the mitochondrial membrane hyperpolarization.

When we analysed the effect of anti-Fas in the 4TO-NOS cell line, we found that the apoptosis inductor caused a lower localization of NOS-3 in the mitochondria. This observation coincided not only with a decrease in the cellular content of nitrated mitochondrial proteins, but also with a non-relevant reduction in respiratory capacity

Table 2
Differentially expressed protein spots between cell lines 4TO and 4TO-NOS (NOS) identified by mass spectrometry. Differential expression ratio in bold indicates statistically significant expression with $p < 0.01$. The rest with $p < 0.05$. In the fold change box 'NOS' indicates 'only expressed in 4TO-NOS'; + indicates anti-Fas treatment.

Biological Classification	Protein name (Accession number)	Molecular function	Spot N°	MS	IS	NOS vs. 4TO	NOS+ vs. 4TO+	4TO+ vs. 4TO	NOS+ vs. NOS
Metabolism	Enoyl-CoA hydratase, mitochondrial (P30084)	β-oxidation	46	589	470	1.3	**1.7**		
	Medium-chain-specific acyl-CoA dehydrogenase mitochondrial (B7Z9I1)		27	379	290	5.4			−1.5
	Short/branched chain-specific acyl-CoA dehydrogenase mitochondrial (B4DQ51)		28	215	155	2.8		**1.4**	
	GAPDH (P04406)	Glycolysis	65	124	77	**2.3**		**3.0**	
	Alpha-enolase (P06733)		18	136	97				1.5
	D-3-phosphoglycerate dehydrogenase (O43175)	Amino acids	8	269	157	−2.1	−1.8		
	Retinal dehydrogenase 1 (P00352)	Retinol	10	651	543	−3.0	−2.0		1.7
	Abhydrolase domain-containing protein 14B (B4DQI4)	Hydrolase	56	72	39	−2.5			2.0
	Sulfurtransferase (J3KPV7)	Transferase	64	264	195	1.5			−1.5
	AMP deaminase 2 (Fragment) (H0Y360)	IMP	104	48				5.2	
	Adenylate kinase 2, mitochondrial (F8VY04)	Energy	109	141	121			1.5	
RNA processing	hnRNPL (P14866)	hnRNP/28S component	4	132	111		−2.8		
			5	206	173		−1.9		
	hnRNPH (P31943)		12	674	569	−1.6			
	hnRNPD0 (H0YA96)		24	273	229		−1.4		
	hnRNPK (P61978)		50	360	314		−2.1		
	28S RNPS22, mitochondrial (P82650)		63	278	185	2.6			
Protein degradation	Cytosol aminopeptidase (P28838)	Proteolysis/Protein stability	11	573	417	−2.1	−2.0		
	Aminoacylase-1 (Q03154)		25	135	79		**2.6**	−1.9	
	Serine protease HTRA2, mitochondrial (O43464)		31	249	189		**2.6**		
	Isochorismatase domain-containing protein 2, mitochondrial (Q96AB3)		73	264	217	**3.7**	**2.3**		
	Cathepsin B (P07858)		37	288	204		**1.4**	**1.8**	
			54	407	332		**−1.5**	**1.3**	
	Cathepsin D (P07339)		41	498	389	**NOS**	**NOS+**		
			42	598	475	**2.3**	**2.8**		
			44	268	223	**1.9**	2.1		
Protein processing	60 kDa heat shock protein, mitochondrial (P10809)	Chaperone/Protein assembly	14	130	114		−4.1		−3.7
			15	415	350			−1.2	**−1.5**
			16	136		2.0	**3.9**		
			17	287	210		−1.9		
	78 kDa glucose-regulated protein (P11021)		32	98	78		**2.1**		
			48	513	434		−1.2		**−1.3**
			66	610	463		**−1.8**		
			86	157	140	1.8			−1.4
			93	131	113		**−1.5**		**−1.6**
	Heat shock protein beta-1 (P04792)		47	300	255				**1.8**
	Protein DJ-1 (Q99497)		57	183	102		**1.3**		
	GrpE protein homolog 1, mitochondrial (Q9HAV7)		58	313	271		2.5		
	Stress-70 protein, mitochondrial (P38646)		68	441	386	1.8			
	ATP synthase mitochondrial F1 complex assembly factor 1 (H0YD21)		38	70			**8.4**		3.1
	Calreticulin (P27797)		100	133	107		**−1.5**		
Skeleton	Actin, cytoplasmic 2 (P63261)		26	761	614			**1.7**	
			43	119	103		**1.7**		
	Microtubule-actin cross-linking factor 1, isoforms 1/2/3/5 (F5GZL7)		92	48	11		**−2.6**		
Redox Homeostasis	Thioredoxin (Fragment) (H7BZJ3)	Oxido-reductase/Isomerase	36	148	128	1.4			−1.2
	Thioredoxin-dependent peroxide (E9PH29)		51	353	313	**3.2**	**3.6**		
	NADPH:adrenodoxin oxidoreductase, mitochondrial (P22570)		55	582	506	**3.7**	**3.1**		
	Peroxiredoxin-2 (P32119)		62	800	323	**2.1**	1.4	**1.7**	
	Peroxiredoxin-1 (Q06830)		72	407	279			**2.0**	
	SOD [Mn] mitochondrial (P04179)		74	450	375	**3.2**			
	Aldo-keto reductase family 1 member C1 (Q04828)		85	328	258	**6.9**	2.0	2.8	
	Protein disulfide isomerase family A, member 3, isoformCRA_b (G5EA52)		9	943	636		**−5.1**	**3.7**	
			13	350	266		**−2.1**		−1.7
			67	406	299			**1.9**	
	Protein disulfide-isomerase (H7BZ94)		30	196	149	−2.4			
	Protein disulfide-isomerase (I3L2P8)		107		91	−2.4			

and the complex I-dependent oxygen consumption. As expected, NOS-3 overexpressing cells showed increased susceptibility to anti-Fas-induced cell death, which was mediated by the activity increase of caspase-9 and caspase-3. By contrast, apoptosis induction in the control cell line 4TO was only related to the increase of caspase-3 activity. Therefore, while in the control cell line anti-Fas induced apoptosis through the extrinsic pathway, an additional activation of both the extrinsic and the mitochondrial apoptotic pathways was observed in 4TO-NOS, which was higher than that induced by NOS-3 overexpression alone.

In order to identify intermediates that could be involved in the process of cell death in 4TO-NOS, we analysed the protein expression profile compared to the control cell line 4TO. We identified proteins with different biological functions, whose differential expression is
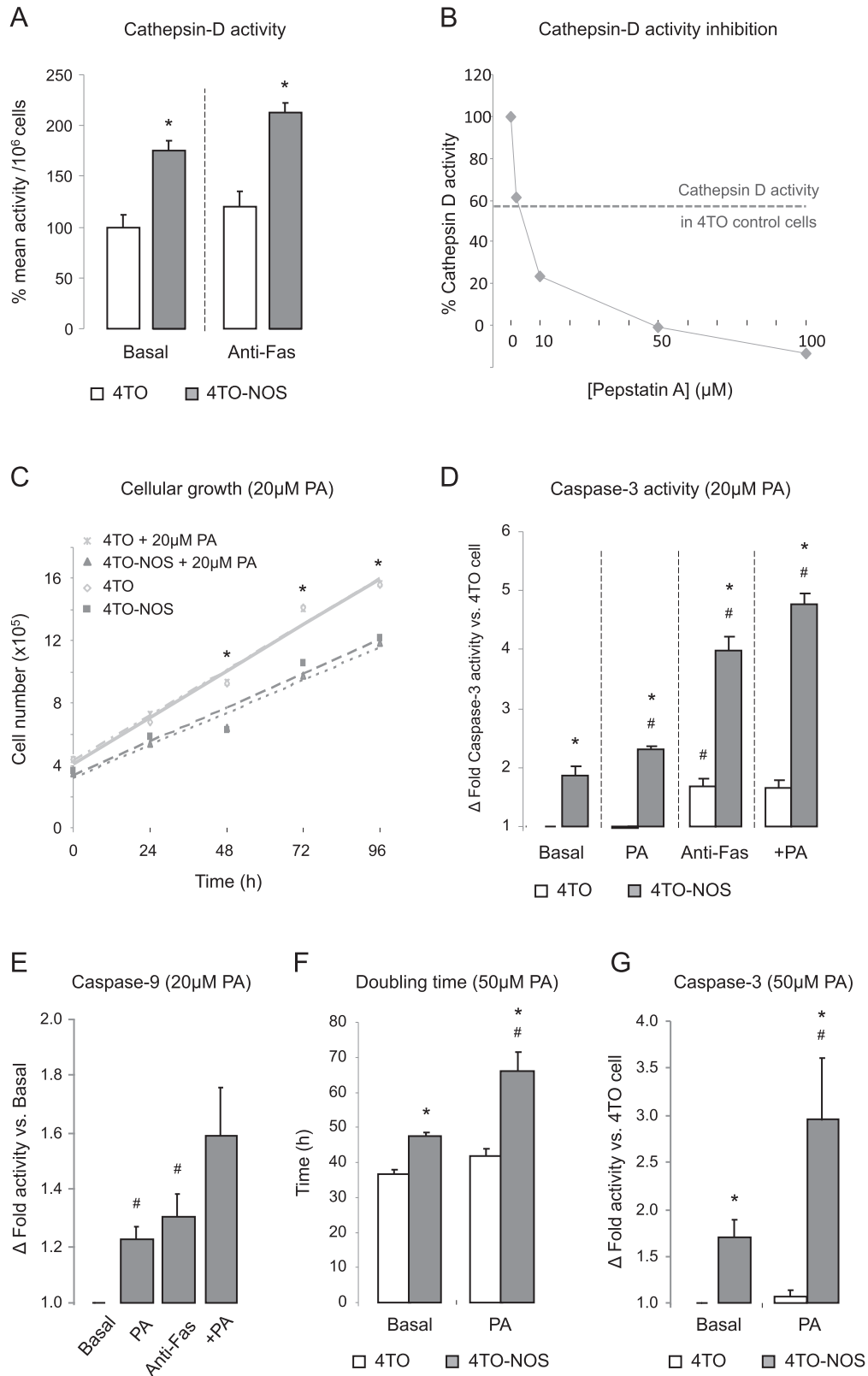
Fig. 6. Cathepsin D activity and cell death. (A) CatD activity in cell lysates (n = 4). (B) CatD activity inhibition curve by pepstatin A. Normal CatD activity in control cell line 4TO is marked. (C) Effect of 20 μM pepstatin A on cell growth (n = 3) and (D) caspase-3 (n = 3) and (E) caspase-9 (n = 3) activities. (F) Effect of 50 μM pepstatin A on cell growth (n = 4) and (G) caspase-3 activity (n = 5) at 48 h. +PA indicates treatment with pepstatin A (PA) plus anti-Fas. Data are mean ± SEM. Statistically significant differences between cell lines* or between treatments[#] are marked.

associated with the reduction of cell growth. Regarding the group of metabolic proteins, it should be noted that nitrosylation is a posttranslational modification by which NO can reversibly regulate β-oxidation [24] and glycolysis [25]. In particular, GAPDH activity may be regulated by nitrosylation, being its hyperactivation an adaptive pro-survival response under pro-oxidant conditions [26]. By contrast, nitrosylated
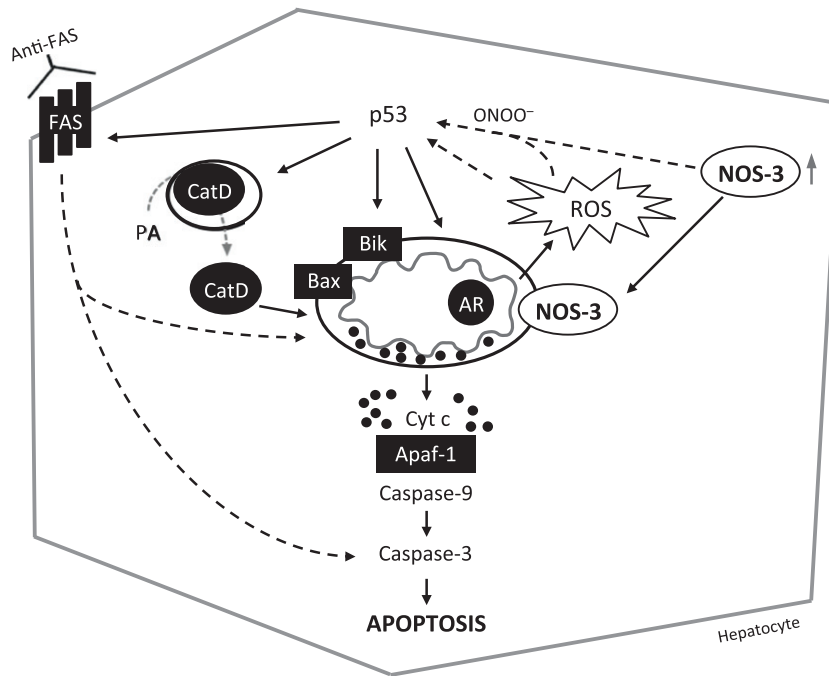
Fig. 7. Cell death mechanisms in 4TO-NOS cells. NOS-3 overexpression was associated with cellular nitro-oxidative stress through the respiratory capacity increase of mitochondrial complex II + III and the tyrosine nitration of mitochondrial proteins. Nitro-oxidative stress induced by NOS-3 overexpression in HepG2 cells was related to 1) the activation of the mitochondrial-associated caspase pathway through the expression increase of pro-apoptotic genes and the release of cyt c into the cytoplasm; 2) the expression increase of proteins adrenodoxin reductase mitochondrial (AR) and cathepsin D (CatD); and 3) higher susceptibility to anti-FAS induced cell death through activation of the apoptosis pathways. The expression regulation of these factors including Bax, Bik, Apaf-1, AR, CatD and FAS, has been previously related to p53, which is upregulated in 4TO-NOS cells. Both, ROS production and protein tyrosine-nitration have been associated with p53 regulation and apoptosis. AR may contribute to oxidative stress. Pepstatin A (PA) induces apoptosis likely through the release of CatD from lysosomes.

GAPDH is able to be transferred to the nucleus and to activate p53, leading to cell death [27]. In this regard, we have previously reported that NOS-3 overexpression increases the profile of S-nitrosylated proteins [14], and induces p53 expression in HepG2 [10], reducing cell survival. Adding anti-Fas to the cell culture induced GAPDH expression in the control cell line, thus abolishing the difference induced by NOS-3 overexpression.

In the second largest group of identified proteins, we found over-expression of proteins involved in the cellular antioxidant system. This agreed with the gene expression profile of 4TO-NOS. Thus, the up-regulation of antioxidant enzymes through activation of the ROS-sensitive signalling pathway is well established. Peroxiredoxins are involved in the attenuation of the generation of reactive oxygen/nitrogen species and NO [28,29], and may be regulated by nitrosylation [30]. Moreover, we detected a significant increase of AR in the 4TO-NOS cell line. AR is a mitochondrial oxidoreductase that catalyses the oxidation of NADPH, acting as the first electron transfer protein of mitochondrial P450 systems. This system can work as a futile NADPH oxidase, oxidizing NADPH in the absence of substrate, leaking electrons to O_2 and generating ROS [31]. AR was particularly interesting because it participates in the p53-mediated apoptosis by oxidative stress [32]. Here, increase of AR expression induced by NOS-3 overexpression coincided with ROS production, p53 accumulation [10], and apoptosis induction through the expression of pro-apoptotic genes that are regulated by p53. In agreement with the oxidative status of the cell lines, anti-Fas did not change the expression profile of AR in 4TO and 4TO-NOS.

The protease CatD was identified in two up-regulated spots, as well as in a third additional spot only detected in 4TO-NOS, which probably belongs to a chemical modification of the protein. Indeed the posttranslational modification of CatD has been implicated in tissue remodelling occurring after lactation [33]. In accordance with the protein expression analysis, the stable overexpression of NOS-3 increased the CatD activity in HepG2 cells. These results were also related to p53 expression [10,34]

and agree with previous observations in which CatD participated in the apoptosis induction by NO [35]. Furthermore, it has been reported that the genetic and pharmacological inhibition of CatD is effective in blocking apoptosis in several different models, including anti-Fas in-duced cell death [36]. Despite this, anti-Fas did not induce CatD activity in the control cell line 4TO. To better understand the role of CatD in our cell model of NOS-3 overexpression, we analysed cell death-related parameters in the presence of pepstatin A. At 20 μM, pepstatin A was able to inhibit CatD activity in 4TO-NOS below the observed level in the control cell line 4TO. However, it did not affect the growth of 4TO or 4TO-NOS cells. As expected, 20 μM pepstatin A failed to suppress the caspase-3 activity induced by anti-Fas in 4TO control cells, thus indicating that CatD activity is not essential for Fas-induced cell death in HepG2. These results differ from those previously published about the participation of the protease in apoptotic systems triggered by the activation of cell surface receptors [36,37]. On the other hand, CatD activity inhibition in 4TO-NOS caused a significant increase in the caspase-3 activity, which was significantly higher to that caused by the NOS-3 overexpression at both in basal conditions and after anti-Fas addition. Thus, CatD activity induced by NOS-3 overexpression seemed to be associated with an anti-apoptotic effect rather than pro-apoptotic. In this regard, an anti-apoptotic role for CatD cannot be ex-cluded since it is overexpressed in many malignant tumours and it is as-sociated with cancer spreading and clinical outcome, and its expression is conditional on apoptosis-associated protein phenotype [38]. Furthermore, the protease may promote cell survival under oxidative stress [39]. Despite of this, Beaujouin et al. reported that CatD overexpression by cancer cells exerts a pro-apoptotic effect that is independent on its catalytic activity. Thus, cytosolic CatD would stimulate apoptosis by interacting with the apoptotic machinery rather than by cleaving specific substrates [40]. If so, we could not rule out a pro-apoptotic role for CatD in our cell model of NOS-3 overexpression since the CatD inhibitor pepstatin A stimulates the protease release from lysosomes at the commonly used dose of 50 μM [41]. In such a scenario, the

caspase-3 activity increase that we observed in 4TO-NOS after pepstatin A administration could be a consequence of a higher cytoplasmic localization of CatD, and not an effect caused by the CatD activity inhibition. This is consistent with the increased caspase-9 activity induced by pepstatin A in NOS-3 overexpressing cells, since inactive pro-caspase-9 is activated through the mitochondrial death pathway. Indeed, 50 μM pepstatin A caused a significant slowing down of cell growth in 4TO-NOS.

In conclusion, NOS-3 overexpression promoted AR and CatD up-regulation in a process related to oxidative stress generation and apoptosis induction. These observations agree with previous studies where both enzymes were associated with apoptosis, and were regulated by p53. Thus, AR and CatD emerge as new targets that could be involved in the reduction of cell survival in NOS-3 overexpressing cells, and join the list of proteins that we previously identified [14]. Overall, NOS-3 overexpression caused a higher sensitivity to anti-Fas-induced cell death through the upregulation of pro-apoptotic genes and the increase in caspase-9 and caspase-3 activities, without affecting AR and CatD activity and/or expression. Since the pro-apoptotic effect of CatD overexpression may not be related to its enzymatic activity, we cannot exclude a significant role for this protein in the apoptosis induction by NOS-3 overexpression. The potential role of the GAPDH increase in the regulation of p53 activity in 4TO-NOS cells remains to be determined. Similarly, it remains to be established the posttranslational modification affecting CatD activity during the NOS-3 overexpression.

Supplementary data to this article can be found online at http://dx.doi.org/10.1016/j.bbamcr.2015.02.015.

Acknowledgments

References

[1] J. Muntane, M. de la Mata, Nitric oxide and cancer, World J. Hepatol. 2 (9) (2010) 337–344. http://dx.doi.org/10.4254/wjh.v2.i9.337.

[2] W.K. Alderton, C.E. Cooper, R.G. Knowles, Nitric oxide synthases: structure, function and inhibition, Biochem. J. 357 (Pt 3) (2001) 593–615. http://dx.doi.org/10.1042/0264-6021:3570593.

[3] S. Gao, J. Chen, S.V. Brodsky, H. Huang, S. Adler, J.H. Lee, N. Dhadwal, L. Cohen-Gould, S.S. Gross, M.S. Goligorsky, Docking of endothelial nitric oxide synthase (eNOS) to the mitochondrial outer membrane: a pentabasic amino acid sequence in the autoinhibitory domain of eNOS targets a proteinase K-cleavable peptide on the cytoplasmic face of mitochondria, J. Biol. Chem. 279 (16) (2004) 15968–15974. http://dx.doi.org/10.1074/jbc.M308504200.

[4] A.J. Kanai, L.L. Pearce, P.R. Clemens, L.A. Birder, M.M. VanBibber, S.Y. Choi, W.C. de Groat, J. Peterson, Identification of a neuronal nitric oxide synthase in isolated cardiac mitochondria using electrochemical detection, Proc. Natl. Acad. Sci. U. S. A. 98 (24) (2001) 14126–14131. http://dx.doi.org/10.1073/pnas.241380298.

[5] S.L. Elfering, T.M. Sarkela, C. Giulivi, Biochemistry of mitochondrial nitric-oxide synthase, J. Biol. Chem. 277 (41) (2002) 38079–38086. http://dx.doi.org/10.1074/jbc.M205256200.

[6] C. Villanueva, C. Giulivi, Subcellular and cellular locations of nitric oxide synthase isoforms as determinants of health and disease, Free Radic. Biol. Med. 49 (3) (2010) 307–316. http://dx.doi.org/10.1016/j.freeradbiomed.2010.04.004.

[7] S. Diaz-Troya, S. Najib, V. Sanchez-Margalet, eNOS, nNOS, cGMP and protein kinase G mediate the inhibitory effect of pancreastatin, a chromogranin A-derived peptide, on growth and proliferation of hepatoma cells, Regul. Pept. 125 (1–3) (2005) 41–46. http://dx.doi.org/10.1016/j.regpep.2004.07.031.

[8] N.A. Riobo, E. Clementi, M. Melani, A. Boveris, E. Cadenas, S. Moncada, J.J. Poderoso, Nitric oxide inhibits mitochondrial NADH:ubiquinone reductase activity through peroxynitrite formation, Biochem. J. 359 (Pt 1) (2001) 139–145. http://dx.doi.org/10.1042/0264-6021:3590139.

[9] P. Sarti, E. Forte, D. Mastronicola, A. Giuffre, M. Arese, Cytochrome c oxidase and nitric oxide in action: molecular mechanisms and pathophysiological implications, Biochim. Biophys. Acta 1817 (4) (2012) 610–619. http://dx.doi.org/10.1016/j.bbabio.2011.09.002.

[10] R. Gonzalez, G. Ferrin, P. Aguilar-Melero, I. Ranchal, C.I. Linares, R.I. Bello, M. de la Mata, V. Gogvadze, J.A. Barcena, J.M. Alamo, S. Orrenius, F.J. Padillo, B. Zhivotovsky, J. Muntane, Targeting hepatoma using nitric oxide donor strategies, Antioxid. Redox Signal. 18 (5) (2013) 491–506. http://dx.doi.org/10.1089/ars.2011.4476.

[11] J. Ogasawara, R. Watanabe-Fukunaga, M. Adachi, A. Matsuzawa, T. Kasugai, Y. Kitamura, N. Itoh, T. Suda, S. Nagata, Lethal effect of the anti-Fas antibody in mice, Nature 364 (6440) (1993) 806–809. http://dx.doi.org/10.1038/364806a0.

[12] D.C. Huang, M. Hahne, M. Schroeter, K. Frei, A. Fontana, A. Villunger, K. Newton, J. Tschopp, A. Strasser, Activation of Fas by FasL induces apoptosis by a mechanism that cannot be blocked by Bcl-2 or Bcl-x(L), Proc. Natl. Acad. Sci. U. S. A. 96 (26) (1999) 14871–14876. http://dx.doi.org/10.1073/pnas.96.26.14871.

[13] B. Rigas, J.L. Williams, NO-donating NSAIDs and cancer: an overview with a note on whether NO is required for their action, Nitric Oxide 19 (2) (2008) 199–204. http://dx.doi.org/10.1016/j.niox.2008.04.022.

[14] P. Aguilar-Melero, G. Ferrin, J. Muntane, Effects of nitric oxide synthase-3 overexpression on post-translational modifications and cell survival in HepG2 cells, J. Proteome 75 (3) (2012) 740–755. http://dx.doi.org/10.1016/j.jprot.2011.09.010.

[15] R. Gonzalez, G. Ferrin, A.B. Hidalgo, I. Ranchal, P. Lopez-Cillero, M. Santos-Gonzalez, G. Lopez-Lluch, J. Briceno, M.A. Gomez, A. Poyato, J.M. Villalba, P. Navas, M. de la Mata, J. Muntane, N-acetylcysteine, coenzyme Q10 and superoxide dismutase mimetic prevent mitochondrial cell dysfunction and cell death induced by d-galactosamine in primary culture of human hepatocytes, Chem. Biol. Interact. 181 (1) (2009) 95–106. http://dx.doi.org/10.1016/j.cbi.2009.06.003.

[16] R. Acin-Perez, M.P. Bayona-Bafaluy, M. Bueno, C. Machicado, P. Fernandez-Silva, A. Perez-Martos, J. Montoya, M.J. Lopez-Perez, J. Sancho, J.A. Enriquez, An intragenic suppressor in the cytochrome c oxidase I gene of mouse mitochondrial DNA, Hum. Mol. Genet. 12 (3) (2003) 329–339. http://dx.doi.org/10.1093/hmg/ddg021.

[17] R. Moreno-Loshuertos, G. Ferrin, R. Acin-Perez, M.E. Gallardo, C. Viscomi, A. Perez-Martos, M. Zeviani, P. Fernandez-Silva, J.A. Enriquez, Evolution meets disease: penetrance and functional epistasis of mitochondrial tRNA mutations, PLoS Genet. 7 (4) (2011) e1001379. http://dx.doi.org/10.1371/journal.pgen.1001379.

[18] R. Govers, L. Bevers, P. de Bree, T.J. Rabelink, Endothelial nitric oxide synthase activity is linked to its presence at cell–cell contacts, Biochem. J. 361 (Pt 2) (2002) 193–201. http://dx.doi.org/10.1042/0264-6021:3610193.

[19] H.C. Lee, Y.H. Wei, Mitochondrial biogenesis and mitochondrial DNA maintenance of mammalian cells under oxidative stress, Int. J. Biochem. Cell Biol. 37 (4) (2005) 822–834. http://dx.doi.org/10.1016/j.biocel.2004.09.010.

[20] E. Nisoli, E. Clementi, C. Paolucci, V. Cozzi, C. Tonello, C. Sciorati, R. Bracale, A. Valerio, M. Francolini, S. Moncada, M.O. Carruba, Mitochondrial biogenesis in mammals: the role of endogenous nitric oxide, Science 299 (5608) (2003) 896–899. http://dx.doi.org/10.1126/science.1079368.

[21] M.P. Murphy, How mitochondria produce reactive oxygen species, Biochem. J. 417 (1) (2009) 1–13. http://dx.doi.org/10.1042/BJ20081386.

[22] E.S. Han, F.L. Muller, V.I. Perez, W. Qi, H. Liang, L. Xi, C. Fu, E. Doyle, M. Hickey, J. Cornell, C.J. Epstein, L.J. Roberts, H. Van Remmen, A. Richardson, The in vivo gene expression signature of oxidative stress, Physiol. Genomics 34 (1) (2008) 112–126. http://dx.doi.org/10.1152/physiolgenomics.00239.2007.

[23] S. Haupt, M. Berger, Z. Goldberg, Y. Haupt, Apoptosis — the p53 network, J. Cell Sci. 116 (Pt 20) (2003) 4077–4085. http://dx.doi.org/10.1242/jcs.00739.

[24] P.T. Doulias, M. Tenopoulou, J.L. Greene, K. Raju, H. Ischiropoulos, Nitric oxide regulates mitochondrial fatty acid metabolism through reversible protein S-nitrosylation, Sci. Signal. 6 (256) (2013) rs1. http://dx.doi.org/10.1126/scisignal.2003252.

[25] M. Zaffagnini, S. Morisse, M. Bedhomme, C.H. Marchand, M. Festa, N. Rouhier, S.D. Lemaire, P. Trost, Mechanisms of nitrosylation and denitrosylation of cyto-plasmic glyceraldehyde-3-phosphate dehydrogenase from Arabidopsis thaliana, J. Biol. Chem. 288 (31) (2013) 22777–22789. http://dx.doi.org/10.1074/jbc.M113.475467.

[26] C. Cerella, M. D'Alessio, S. Cristofanon, M. De Nicola, F. Radogna, M. Dicato, M. Diederich, L. Ghibelli, Subapoptogenic oxidative stress strongly increases the activity of the glycolytic key enzyme glyceraldehyde 3-phosphate dehydrogenase, Ann. N. Y. Acad. Sci. 1171 (2009) 583–590. http://dx.doi.org/10.1111/j.1749-6632.2009.04723.x.

[27] N. Sen, M.R. Hara, M.D. Kornberg, M.B. Cascio, B.I. Bae, N. Shahani, B. Thomas, T.M. Dawson, V.L. Dawson, S.H. Snyder, A. Sawa, Nitric oxide-induced nuclear GAPDH activates p300/CBP and mediates apoptosis, Nat. Cell Biol. 10 (7) (2008) 866–873. http://dx.doi.org/10.1038/ncb1747.

[28] M. Reinartz, Z. Ding, U. Flogel, A. Godecke, J. Schrader, Nitrosative stress leads to protein glutathiolation, increased s-nitrosation, and up-regulation of peroxiredoxins in the heart, J. Biol. Chem. 283 (25) (2008) 17440–17449. http://dx.doi.org/10.1074/jbc.M800126200.

[29] H.N. Sun, S.U. Kim, S.M. Huang, J.M. Kim, Y.H. Park, S.H. Kim, H.Y. Yang, K.J. Chung, T.H. Lee, H.S. Choi, J.S. Min, M.K. Park, S.K. Kim, S.R. Lee, K.T. Chang, S.H. Lee, D.Y. Yu, D.S. Lee, Microglial peroxiredoxin V acts as an inducible anti-inflammatory antioxidant through cooperation with redox signaling cascades, J. Neurochem. 114 (1) (2010) 39–50. http://dx.doi.org/10.1111/j.1471-4159.2010.06691.x.

[30] J. Fang, T. Nakamura, D.H. Cho, Z. Gu, S.A. Lipton, S-nitrosylation of peroxiredoxin 2 promotes oxidative stress-induced neuronal cell death in Parkinson's disease, Proc. Natl. Acad. Sci. U. S. A. 104 (47) (2007) 18742–18747. http://dx.doi.org/10.1073/pnas.0705904104.

[31] I. Hanukoglu, Antioxidant protective mechanisms against reactive oxygen species (ROS) generated by mitochondrial P450 systems in steroidogenic cells, Drug Metab. Rev. 38 (1–2) (2006) 171–196. http://dx.doi.org/10.1080/03602530600570040.

[32] P.M. Hwang, F. Bunz, J. Yu, C. Rago, T.A. Chan, M.P. Murphy, G.F. Kelso, R.A. Smith, K.W. Kinzler, B. Vogelstein, Ferredoxin reductase affects p53-dependent, 5-fluorouracil-induced apoptosis in colorectal cancer cells, Nat. Med. 7 (10) (2001) 1111–1117. http://dx.doi.org/10.1038/nm1001-1111.

[33] R. Zaragoza, L. Torres, C. Garcia, P. Eroles, F. Corrales, A. Bosch, A. Lluch, E.R. Garcia-Trevijano, J.R. Vina, Nitration of cathepsin D enhances its proteolytic activity during mammary gland remodelling after lactation, Biochem. J. 419 (2) (2009) 279–288. http://dx.doi.org/10.1042/BJ20081746.

[34] G.S. Wu, P. Saftig, C. Peters, W.S. El-Deiry, Potential role for cathepsin D in p53-dependent tumor suppression and chemosensitivity, Oncogene 16 (17) (1998) 2177–2183. http://dx.doi.org/10.1038/sj.onc.1201755.

[35] C.M. Pilane, E.F. LaBelle, NO induced apoptosis of vascular smooth muscle cells accompanied by ceramide increase, J. Cell. Physiol. 199 (2) (2004) 310–315. http://dx.doi.org/10.1002/jcp.10464.

[36] L.P. Deiss, H. Galinka, H. Berissi, O. Cohen, A. Kimchi, Cathepsin D protease mediates programmed cell death induced by interferon-gamma, Fas/APO-1 and TNF-alpha, EMBO J. 15 (15) (1996) 3861–3870.

[37] H. Malhi, M.E. Guicciardi, G.J. Gores, Hepatocyte death: a clear and present danger, Physiol. Rev. 90 (3) (2010) 1165–1194. http://dx.doi.org/10.1152/physrev.00061. 2009.

[38] C. Fan, X. Lin, E. Wang, Clinicopathological significance of cathepsin D expression in non-small cell lung cancer is conditional on apoptosis-associated protein phenotype: an immunohistochemistry study, Tumour Biol. 33 (4) (2012) 1045–1052. http://dx.doi.org/10.1007/s13277-012-0338-y.

[39] Y.S. Hah, H.S. Noh, J.H. Ha, J.S. Ahn, J.R. Hahm, H.Y. Cho, D.R. Kim, Cathepsin D inhibits oxidative stress-induced cell death via activation of autophagy in cancer cells, Cancer Lett. 323 (2) (2012) 208–214. http://dx.doi.org/10.1016/j.canlet.2012. 04.012.

[40] M. Beaujouin, S. Baghdiguian, M. Glondu-Lassis, G. Berchem, E. Liaudet-Coopman, Overexpression of both catalytically active and -inactive cathepsin D by cancer cells enhances apoptosis-dependent chemo-sensitivity, Oncogene 25 (13) (2006) 1967–1973. http://dx.doi.org/10.1038/sj.onc.1209221.

[41] L. Emert-Sedlak, S. Shangary, A. Rabinovitz, M.B. Miranda, S.M. Delach, D.E. Johnson, Involvement of cathepsin D in chemotherapy-induced cytochrome c release, caspase activation, and cell death, Mol. Cancer Ther. 4 (5) (2005) 733–742. http://dx.doi.org/10.1158/1535-7163.MCT-04-0301.